Hybrid Decoding of Both Spikes and Low-Frequency Local Field Potentials for Brain-Machine Interfaces

Sergey D. Stavisky-*EMBS Student Member*, Jonathan C. Kao-*EMBS Student Member*,
Paul Nuyujukian-*EMBS Member,* Stephen I. Ryu-*IEEE Member*,
and Krishna V. Shenoy, *IEEE Senior Member*

***Abstract*— The best-performing brain-machine interfaces (BMIs) to date decode movement intention from intracortically recorded spikes, but these signals may be lost over time. A way to increase the useful lifespan of BMIs is to make more comprehensive use of available neural signals. Recent studies have demonstrated that the local field potential (LFP), a potentially more robust signal, can also be used to control a BMI. However, LFP-driven performance has fallen short of the best spikes-driven performance. Here we report a biomimetic BMI driven by low-frequency LFP that enabled a rhesus monkey to acquire and hold randomly placed targets with 99% success rate. Although LFP-driven performance was still worse than when decoding spikes, to the best of our knowledge this represents the highest-performing LFP-based BMI. We also demonstrate a new hybrid BMI that decodes cursor velocity using both spikes and LFP. This hybrid decoder improved performance over spikes-only decoding. Our results suggest that LFP can complement spikes when spikes are available or provide an alternative control signal if spikes are absent.**

I. Introduction

Brain-machine interfaces (BMIs) are being developed to serve as assistive devices for individuals with movement disabilities. The best-performing BMIs to date have decoded movement intention from multiunit spike activity [1], and BMIs driven by spikes recorded from a similar type of intracortical multielectrode array are now being used by people enrolled in clinical trials to control a computer cursor [2], [3] or robotic limb [4]. Over time arrays often lose their ability to record well-isolated spikes [5], [6], thereby seemingly limiting the BMI's useful lifespan. However, the recent proposition to decode threshold crossings (i.e. accept all sufficiently large neural action potentials but make no attempt to 'sort' them into single-neuron activity [7], [8]) has been used to demonstrate record levels of performance at least 4.5 years after array implantation [1]. But what about electrodes that are unable to provide either single-neuron or multiunit spikes? And what happens ten years after implantation when possibly few, if any, channels are able to record spikes? Fortunately, numerous offline studies, such as [9], [10], have shown that reach kinematics can be decoded from another neural signal, the local field potential (LFP), which is available from the same sensor. LFP can be informative about kinematics even when recorded from electrodes that do not record spikes [11], [12]. More recent studies have demonstrated closed-loop LFP-driven cursor control [13], [14]. Although these LFP-driven BMIs did not achieve target acquisition success rates as high as those previously shown with state-of-the-art spikes decoders [1], [15], they are an encouraging indication that LFP may provide an alternative BMI control signal.

Offline decoding studies have also suggested that BMI performance can be improved by decoding both spikes and LFP together using a hybrid decoder [9], [10]. One closed-loop study [16] has used LFP as a binary 'go' signal after which intended target was decoded from spikes alone. However, closed-loop control of cursor kinematics using a hybrid decoder has not previously been tested.

In this study we evaluated cursor control using both LFP-only and hybrid BMI designs based on decoding the motor-evoked potential (MEP) recorded on two 96-electrode arrays. The MEP, which is a low-frequency LFP feature, is highly unlikely to be contaminated by spikes [17] and therefore is a good candidate neural feature both for providing an alternative neural signal when spikes are absent and for providing an additional source of information to augment spikes as part of a hybrid decoder. We found that the LFP-driven BMI enabled a monkey to perform two different target acquisition tasks at over 98% success rate. Furthermore, we found that incorporating LFP into a hybrid decoder increased performance when compared to a state-of-the-art spikes-only decoder.

II. Methods

A. Behavioral Tasks

All procedures and experiments were approved by the Stanford University Institutional Animal Care and Use Committee. A rhesus macaque (monkey R) was trained to perform 2D target acquisition tasks by controlling a cursor with either his hand position or via a BMI. He was free to move his arm even during BMI use. Our *Radial 8 Task* was modeled after the task described in [18]. Targets alternated between the center of the workspace and one of eight pseudorandomly selected locations equally spaced along a 13 cm diameter circle. A liquid reward was given after each successful trial in which the cursor was held inside a 3.4 cm wide acquisition area for a 300 ms hold period. The trial time limit was 8 s, and only trials from the center to one of the eight peripheral targets were analyzed. In the *Random Target Task* targets appeared randomly anywhere in a 20 x 20 cm

Research supported by National Science Foundation Graduate Research Fellowship (S.D.S., J.C.K.), Stanford Medical Scientist Training Program (P.N.), NSF IGERT (S.D.S), NIH Pioneer Award 8DP1HD075623, NIH T-RO1 award NS076460, and DARPA REPAIR award N66001-10-C-2010 (K.V.S.).

S. D. Stavisky (e-mail: sergey.stavisky@stanford.edu), J. C. Kao, P. Nuyujukian, & K. V. Shenoy are at Stanford University, Stanford, CA 94305.

S. I. Ryu is at Palo Alto Medical Foundation, Palo Alto, CA.

978-1-4244-7929-0/14/$26.00 ©2014 IEEE

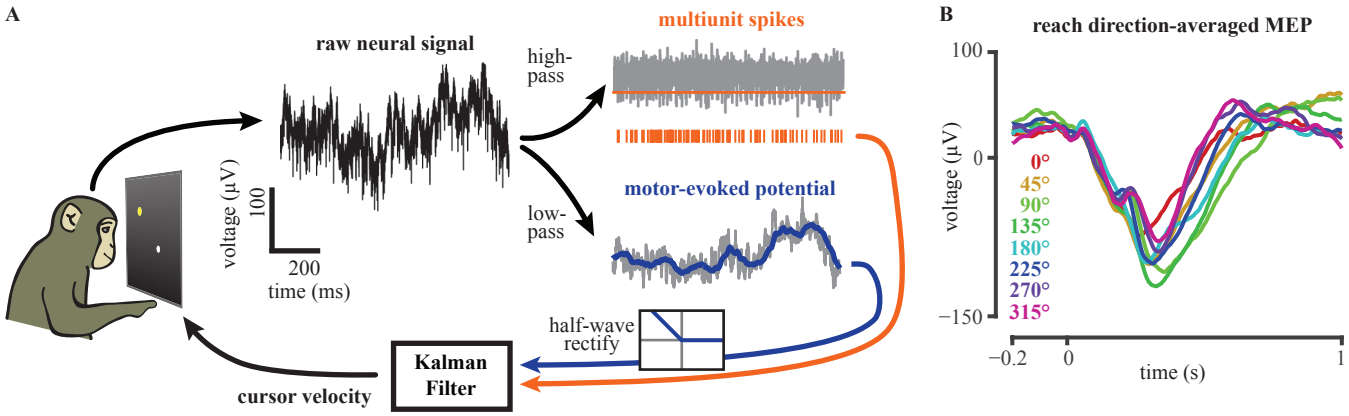

Fig. 1. (A) Overview of the hybrid spikes- and LFP-driven BMI. Raw neural data (black) is recorded from 96-electrode arrays in M1 and PMd. To extract multiunit spikes (orange ticks), the raw data is first high-pass filtered (top right, gray). A spike is then detected whenever this signal crosses below a threshold (orange line). LFP (bottom right, gray) is obtained by low-pass filtering the raw data. The MEP feature (blue) is then extracted by applying a 50 ms boxcar filter to the LFP. Cursor velocity is decoded from both MEP and spikes via a Kalman filter. (B) Example MEP recorded in PMd during arm reaches in eight different directions. Each trace corresponds to the average of 32 reaches. The target was presented at time 0. Dataset R-2013-07-30, elec. 174.

region immediately following the end of the previous trial. The monkey had up to 8 s to hold the cursor inside a 5 cm wide acquisition area for 500 ms.

B. Neural Recording and Signal Processing

Monkey R was implanted with two 96-electrode arrays (1 mm electrodes spaced 400 μm apart; Blackrock Microsystems) using standard neurosurgical techniques [15] 24-25 months prior to this study. One array was implanted into primary motor cortex (M1) and the other into dorsal premotor cortex (PMd) contralateral to the reaching arm. Voltage signals from each of the 192 electrodes were band-pass filtered from 0.3 to 7500 Hz and then processed to obtain both multiunit spikes and MEP (Fig. 1). To extract spikes, the raw signal was first band-pass filtered from 250 to 7500 Hz. A spike was then detected whenever the voltage crossed below a threshold set at the beginning of each day to be -4.5 × rms voltage. LFP was obtained by low-pass filtering the raw data below 500 Hz and clipping samples exceeding ±300 μV to mitigate intermittent noise. MEP was then computed by taking the mean LFP voltage from the previous 50 ms. The specific window length of 50 ms was chosen based on offline decoding and pilot closed-loop experiments; however, performance differed only slightly across the 25 to 200 ms windows which we tested. In pilot studies we also found that an additional step was needed to improve closed-loop cursor control. The positive MEP 'after-potential' following a reach (visible at around t = 0.6 s in Fig. 1B) caused the cursor to 'spring back' in the opposite direction shortly after movement was initiated. We addressed this problem by applying a half-wave rectification step where positive MEP values were set to zero while negative values were passed through.

C. Neural Decoding

At the start of each experiment we collected a training dataset of 500 arm-controlled Radial 8 Task trials using targets located 12 cm from the center. This data was used to train LFP-only, spikes-only, and hybrid velocity Kalman Filter (KF) decoders. All three decoders output a velocity command every 50 ms from input consisting of neural data from the previous 50 ms. For LFP-only decoding we trained a standard velocity KF (see [1]) using all of the data in the training dataset. At each time step the neural features, $\mathbf{y}_{LFP}$, were a 192×1 vector of MEP from each channel. When fitting the model we allowed a causal lag offset between LFP and kinematics; regression error was minimized when LFP led kinematics by 100 ms. No lag was applied when the KF was run in closed-loop. To help stabilize the cursor in the workspace during LFP-driven BMI use we added a relatively small 'centering velocity' to the decoded velocity that pointed towards the screen center with magnitude $0.15 \cdot r\ s^{-1}$ where r is the cursor's distance from the center. To avoid giving the LFP decoder an unfair advantage we also tried adding this centering velocity to the spikes-only and hybrid decoders; this did not increase performance.

For spikes-only decoding we used the FIT-KF algorithm [15]. Briefly, FIT-KF is a streamlined version of the ReFIT-KF [1] and improves upon a standard KF by adjusting kinematics of the training data to better match the subject's presumed movement intention. This decoder operated on $\mathbf{y}_{spikes}$, a 192×1 vector of spike counts from the previous 50 ms.

The hybrid decoder was built by simply combining the FIT-KF spikes decoder and the LFP velocity KF. This new decoder operated on a stacked feature vector $\mathbf{y}_{hybrid} = [\mathbf{y}_{spikes}; \mathbf{y}_{LFP}]$ which was mapped to kinematics by a stacked observation matrix $C_{hybrid} = [C_{spikes}; C_{LFP}]$. A combined covariance matrix Q_{hybrid} was then calculated from the training data and C_{hybrid}. We note that the position-feedback innovation of the FIT-KF was applied to $\mathbf{y}_{spikes}$ in the hybrid decoder, but not to $\mathbf{y}_{LFP}$. The hybrid decoder used the same kinematics dynamical state update matrix and noise model as the spikes decoder.

D. Performance Measures

In addition to success rate, the following metrics were used to quantify task performance:

- Targets Per Minute: Number of successful trials divided by the continuous duration of the task.

- Time to Target (TTT) for Radial 8 Task: Time elapsed between trial start and successful target acquisition, not including the required hold time.
- Normalized TTT for Random Target Task: TTT divided by the straight-line distance between the current and previous target [14].
- Index of Performance (IP): A throughput metric inspired by Fitts' law,

  IP = ID / TTT, where $\mathrm{ID} = \log_2\left(\frac{\mathrm{D}}{\mathrm{W}} + 1\right)$

  is the Index of Difficulty and depends on the reach distance, D, and target width W [13]. Faster acquisition of further and/or smaller targets yields higher IP.

E. *Contribution of LFP and Spikes to Hybrid Decode*

LFP's and spikes' respective contributions to decoded velocity during use of the hybrid BMI were visualized by evaluating, at each 50 ms decode time step, the kinematic state estimate of the KF [19] when the input neural feature is either [**0**; $\mathbf{y}_{\mathrm{LFP}}$] or [$\mathbf{y}_{\mathrm{spikes}}$; **0**].

III. Results

A. *High Performance Using an LFP-only Decoder*

We evaluated the subject's performance using an LFP-only decoder on the Random Target Task for nine experiment days and on the Radial 8 Task for six of those days. Across 14,593 trials of the Random Target Task the monkey had a 99% success rate with normalized time to target of 0.14 ± 0.15 s/cm (mean ± std). This corresponds to an Index of Performance of 1.81 bits/s. Fig. 2 shows the LFP-only performance on the Radial 8 Task. Across 1,679 trials the monkey acquired an average of 16.1 targets/min with a success rate of 98%.

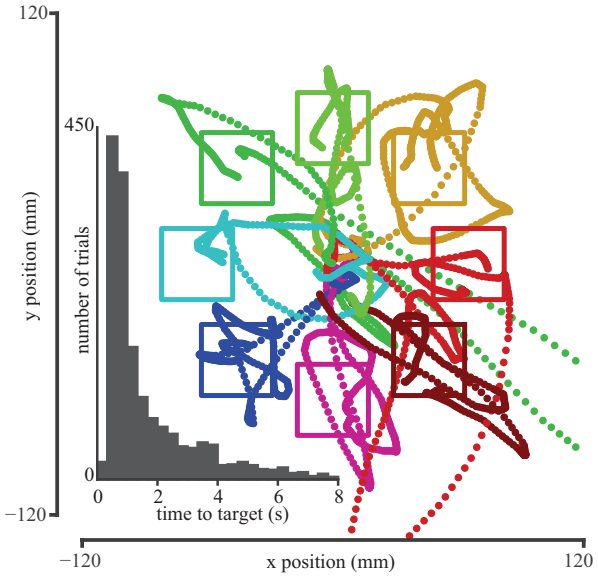

Fig. 2. LFP-only decoder performance on the Radial 8 Task. Example cursor trajectories are shown for sixteen consecutive center out trials (two per target). All sixteen trials were successful. Cursor positions are shown every 10 ms. (Inset) Histogram of times to target for successful trials (98% of total) across six experiment days. Dataset R-2013-09-09.

B. *Hybrid Decoding Outperforms Spikes-only Decoding*

We next evaluated the hybrid BMI. Both LFP and spikes contributed substantially to the decoded velocity, as shown in the example trials in Fig. 3. We compared hybrid decoding to FIT-KF spikes-only decoding on the Random Target Task on each of eight experiment days in an 'ABAB' block design. Across more than 2,000 trials each using the spikes-only and hybrid decoders, both decoders had success rates over 99.9% (difference not significant). As shown in Fig. 3 (inset), normalized times to target were slightly but significantly faster with the hybrid decoder (0.082 ± 0.090 s/cm, mean ± std) than with the spikes-only decoder (0.094 ± 0.072 s/cm; $p < 0.001$, two-tailed t-test). Normalized times to target using both the hybrid and spikes-only decoders were better than with the LFP-only decoder, which was evaluated on a different set of 9 experiment days ($p < 0.001$). Comparing the Index of Performance metric for each decoder yielded the same results.

IV. Discussion

We found LFP to be an inferior but still effective alternative signal to spikes for BMI control. Our LFP-driven decoder enabled faster and more accurate cursor control than the previous best LFP-only performance reported by So and colleagues [13]. On a closely matched task we observed 16.1 target acquisitions per minute at a 98% success rate, compared to the 10.6 targets/min at a 78% success rate achieved by So and colleagues with their best-performing monkey. Between-study differences in monkeys, neural signal quality, and experimental conditions preclude concluding what aspects of our system facilitated its relatively better performance. Nonetheless, we can identify two important novel aspects of our approach. First, we used two 96-channel arrays, compared to twenty channels in [13] and a single 96-channel array in [14]. Second, we decoded

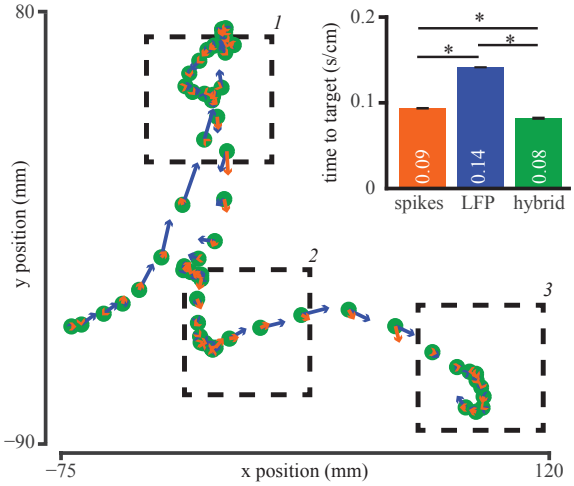

Fig. 3. Hybrid decoder performance. Example cursor trajectories to three consecutive targets during the Random Target Task are shown. Dashed squares represent the target acquisition areas and are numbered chronologically. Cursor position is shown for every 50 ms decode step. At each step we also plot the instantaneous velocity contribution from decoded spikes (orange arrows) and LFP (blue arrows). (Inset) Comparison of BMI performance using each type of decoder. Mean ± SEM normalized times to target across trials from all datasets are shown. * $p < 0.001$. Dataset R-2013-09-28.

only MEP from each electrode, whereas [13] decoded LFP power in multiple bands between 0 and 150 Hz. Flint and colleagues [14] also used MEP in addition to LFP band power, but they had fewer electrodes and did not half-wave rectify their MEP. Further studies that compare different decoding methods in the same animals will be needed to determine the optimal LFP feature(s) for BMIs. A good example of such work is the comparison of using different power bands and number of electrodes in [13].

Furthermore, we've demonstrated that LFP can be combined with spikes in a hybrid decoder to improve BMI performance. While previous studies have used offline results to predict this result, we've now shown that this improvement can indeed be realized during closed-loop control despite presumed differences in controllability between spikes and LFP. To the best of our knowledge this is the first demonstration of closed-loop hybrid decoding of cursor kinematics. However, we observed only a small degree of improvement. This may be because in our study the spikes-only control was already very good and better than LFP-driven control. In future work we will test whether hybrid decoding is more beneficial when fewer channels with good spikes are available, as may be the case with degraded arrays.

Overall, our results demonstrate that even if multielectrode arrays lose their ability to record spikes, as long as low-frequency LFP can still be recorded then it may be possible to combine this LFP with any remaining spikes to maintain high BMI performance. This improved robustness could potentially increase the useful lifespan and clinical viability of motor neural prostheses.

ACKNOWLEDGMENT

We thank M. Mazariegos, M. Wechsler, C. Sherman, & L. Yates for expert surgical assistance & veterinary care, C. Chandrasekaran for Simulink code to access LFP data, B. Oskotsky for IT support, and B. Davis, & E. Casteneda for administrative assistance.

REFERENCES

[1] V. Gilja, P. Nuyujukian, C. A. Chestek, J. P. Cunningham, B. M. Yu, J. M. Fan, M. M. Churchland, M. T. Kaufman, J. C. Kao, S. I. Ryu, and K. V Shenoy, "A high-performance neural prosthesis enabled by control algorithm design," *Nat. Neurosci.*, vol. 15, no. 12, p. 1752, 2012.

[2] L. R. Hochberg, D. Bacher, B. Jarosiewicz, N. Y. Masse, J. D. Simeral, J. Vogel, S. Haddadin, J. Liu, S. S. Cash, P. van der Smagt, and J. P. Donoghue, "Reach and grasp by people with tetraplegia using a neurally controlled robotic arm," *Nature*, vol. 485, no. 7398, pp. 372–375, May 2012.

[3] V. Gilja, C. Pandarinath, C. H. Blabe, L. R. Hochberg, K. V. Shenoy, and J. M. Henderson, "Design and application of a high performance intracortical brain computer interface for a person with amyotrophic lateral sclerosis," in *Society for Neuroscience Annual Meeting*, 2013, vol. 2, p. 80.06.

[4] J. L. Collinger, B. Wodlinger, J. E. Downey, W. Wang, E. C. Tyler-Kabara, D. J. Weber, A. J. C. McMorland, M. Velliste, M. L. Boninger, and A. B. Schwartz, "High-performance neuroprosthetic control by an individual with tetraplegia," *Lancet*, vol. 6736, no. 12, pp. 1–8, Dec. 2012.

[5] J. D. Simeral, S.-P. Kim, M. J. Black, J. P. Donoghue, and L. R. Hochberg, "Neural control of cursor trajectory and click by a human with tetraplegia 1000 days after implant of an intracortical microelectrode array," *J. Neural Eng.*, vol. 8, no. 2, p. 025027, Apr. 2011.

[6] J. C. Barrese, N. Rao, K. Paroo, C. Triebwasser, C. Vargas-Irwin, L. Franquemont, and J. P. Donoghue, "Failure mode analysis of silicon-based intracortical microelectrode arrays in non-human primates.," *J. Neural Eng.*, vol. 10, no. 6, p. 066014, Nov. 2013.

[7] G. W. Fraser, S. M. Chase, A. Whitford, and A. B. Schwartz, "Control of a brain-computer interface without spike sorting.," *J. Neural Eng.*, vol. 6, no. 5, p. 055004, Oct. 2009.

[8] C. A. Chestek, V. Gilja, P. Nuyujukian, J. D. Foster, J. M. Fan, M. T. Kaufman, M. M. Churchland, Z. Rivera-Alvidrez, J. P. Cunningham, S. I. Ryu, and K. V Shenoy, "Long-term stability of neural prosthetic control signals from silicon cortical arrays in rhesus macaque motor cortex," *J. Neural Eng.*, vol. 8, no. 4, p. 045005, Aug. 2011.

[9] C. Mehring, J. Rickert, E. Vaadia, S. Cardoso de Oliveira, A. Aertsen, and S. Rotter, "Inference of hand movements from local field potentials in monkey motor cortex," *Nat. Neurosci.*, vol. 6, no. 12, pp. 1253–4, Dec. 2003.

[10] A. K. Bansal, W. Truccolo, C. E. Vargas-Irwin, and J. P. Donoghue, "Decoding 3D reach and grasp from hybrid signals in motor and premotor cortices: spikes, multiunit activity, and local field potentials," *J. Neurophysiol.*, vol. 107, no. 5, pp. 1337–55, Mar. 2011.

[11] R. D. Flint, E. W. Lindberg, L. R. Jordan, L. E. Miller, and M. W. Slutzky, "Accurate decoding of reaching movements from field potentials in the absence of spikes," *J. Neural Eng.*, vol. 9, no. 4, p. 046006, Jun. 2012.

[12] D. Wang, Q. Zhang, Y. Li, Y. Wang, J. Zhu, S. Zhang, and X. Zheng, "Long-term decoding stability of local field potentials from silicon arrays in primate motor cortex during a 2D center out task.," *J. Neural Eng.*, vol. 11, no. 3, p. 036009, May 2014.

[13] K. So, S. Dangi, A. L. Orsborn, M. C. Gastpar, and J. M. Carmena, "Subject-specific modulation of local field potential spectral power during brain–machine interface control in primates," *J. Neural Eng.*, vol. 11, no. 2, p. 026002, Apr. 2014.

[14] R. D. Flint, Z. A. Wright, M. R. Scheid, and M. W. Slutzky, "Long term, stable brain machine interface performance using local field potentials and multiunit spikes," *J. Neural Eng.*, vol. 10, no. 5, p. 056005, Oct. 2013.

[15] J. M. Fan, P. Nuyujukian, J. C. Kao, C. A. Chestek, S. I. Ryu, and K. V Shenoy, "Intention estimation in brain–machine interfaces," *J. Neural Eng.*, vol. 11, no. 1, p. 016004, 2014.

[16] E. J. Hwang and R. A. Andersen, "Brain control of movement execution onset using local field potentials in posterior parietal cortex," *J. Neurosci.*, vol. 29, no. 45, pp. 14363–14370, Nov. 2009.

[17] S. Waldert, R. N. Lemon, and A. Kraskov, "Influence of spiking activity on cortical local field potentials," *J. Physiol.*, vol. 591, no. 21, pp. 5291–5303, Nov. 2013.

[18] S. Dangi, K. So, A. L. Orsborn, M. C. Gastpar, and J. M. Carmena, "Brain-machine interface control using broadband spectral power from local field potentials," in *35th Annual International Conference of the IEEE EMBS*, 2013, pp. 285–288.

[19] W. Q. Malik, W. Truccolo, E. N. Brown, and L. R. Hochberg, "Efficient decoding with steady-state Kalman filter in neural interface systems.," *IEEE Trans. Neural Syst. Rehabil. Eng.*, vol. 19, no. 1, pp. 25–34, Feb. 2011.